Computer Simulations of Chains End-Grafted onto a Spherical Surface. Effect of Matrix Polymer

Jaroslaw Klos*,†,‡ and Tadeusz Pakula†

Max-Planck-Institute for Polymer Research, Postfach 3148, 55021 Mainz, Germany, and Faculty of Physics, A. Mickiewicz University, Umultowska 85, 61-614 Poznan, Poland

Received January 28, 2004; Revised Manuscript Received August 3, 2004

ABSTRACT: Linear flexible polymers of N_g monomers, end-grafted at the density σ onto a spherical surface of radius R ("hairy sphere"), including the case of a flat impenetrable wall ($R \rightarrow \infty$), are simulated using the cooperative motion algorithm. The simulations have been carried out for a wide range of parameters characterizing the hairy surfaces (N_g, σ, and R) and concern in more detail the influence of length of chains constituting the surrounding medium on the anchored ones. This is achieved by gradual varying the polymerization degree N of the matrix chains between the two extremes of a dense melt of identical chains ($N = N_g$) and a simple solvent consisting of nonbounded beads ($N = 1$). The analysis of the properties of the grafted layer is based on concentration profiles, distributions of polymer centers of mass, and distributions of free ends of chains. Moreover, some of the scaling relations and analytical formulas predicted for grafted chains are tested.

Introduction

The interface between thin films of end-grafted polymers (brushes) and mobile, unconstrained chains has been the subject of intensive experimental and theoretical research due to a rich variety of areas in which such systems can be useful. For instance, the technological applications of grafted layers include dielectrics, biomedical devices, adhesives, paints, and inks. A number of measurement techniques have been used to inspect brushes suspended in polymer matrices in order to tackle such problems as various interactions between these two components, dispersion of anchored random copolymers, and wetting and dewetting phenomena.[1−6]

Conformations of polymers grafted onto a surface both in a pure solvent and in a polymer melt were for the first time discussed theoretically by means of scaling relations and, depending on N_g, N, and σ, provided various concentration profiles for the grafted layer.[7,8] More recently, scaling laws were also used to describe the dependencies of brush thickness on system parameters and to study the penetration phenomena on the interface between the brush and surrounding melt.[9−11] Furthermore, the most detailed and quantitative information on the above issues to date has been obtained by self-consistent-field (SCF) approaches and mean-field theories that, among others, bring about a parabolic concentration profile of the grafted chains in a pure solvent.[12−22] Chain dynamics and static properties in polymer brushes that are in contact with a solution of the same polymers have also been examined using computer simulations.[23−26]

In this paper we complement the simulation studies of interaction of a spherical particle with linear chains.[25,26] In particular, we continue our interests in polymers permanently grafted to a spherical surface with one of their ends and consider in more detail the effect of variable polymerization degree of the surrounding matrix chains on the anchored ones. To the best of our knowledge, the question of polymers end-grafted to curved surfaces under melt conditions is, unlike the case of flat interfaces, of poorer documentation in the literature.[27−30] Refs 29 and 30 are concerned with the interactions between relatively large hairy spheres immersed in a melt of chemically identical and different chains. The curvature of the particles is taken into account by incorporating the so-called Derjaguin approximation, whereas in ref 28 Alexander−de Gennes scaling ideas are adapted to describe conformations of stars in high molecular mass solvents. Also, molecular dynamics simulation studies of polymers end-grafted to a flat surface and immersed in a melt of free chains have been performed.[31]

Here, both spherical and flat brushes are revisited by performing lattice Monte Carlo simulations. As in the previous papers,[25,26] we benefit from the cooperative motion algorithm (CMA) that enables to investigate systems both in the extreme of very high value of the surface coverage and monomer concentrations.[32] In particular, this algorithm has successfully been applied in the studies of a variety of systems of polymer melts confined between parallel walls where both qualitative and quantitative results have been obtained. Actually, among others, the latter include correct chain length dependencies of the mean-squared end-to-end distance and the mean-squared radius of gyration. Furthermore, a good agreement between the simulated results and the predictions of the self-consistent-field theory has been found.[33−35]

In this paper, the simulations are performed for grafted layers immersed in various matrices consisting of chemically identical polymer species. The type of the matrix is varied by keeping the length of the grafted chains N_g constant and gradually changing that of the medium ones N from the situation in a dense melt ($N = N_g$) to that in a simple solvent represented by single beads ($N = 1$). The static properties of the layer are considered, and the results characterizing its configurations are reported. Since the only interaction present

† Max-Planck-Institute for Polymer Research.
‡ A. Mickiewicz University.
* To whom correspondence should be addressed: Ph +48 61 829 5072; Fax +48 61 8257758; e-mail klos@zawrat.amu.edu.pl.

10.1021/ma049818l CCC: $27.50
Published on Web 09/25/2004

is the excluded volume, all of the recorded effects are athermal.

Model and Numerical Procedure

The systems considered here consist of free and end-grafted linear chains modeled on the face-centered-cubic lattice with periodic boundary conditions. A linear chain, in turn, is made out of N successive beads connected by rigid bonds of length $a = c/\sqrt{2}$, where c is the lattice constant. The length unit chosen here is $c/2$. Furthermore, the configurations are tossed using the cooperative motion algorithm (CMA) in which one simulation step is carried out by shifting both single beads and chain elements collectively along a randomly generated closed loop. A part of the chain is considered movable if its local conformation can be changed by subsequent translating of one or a few beads, each by one lattice site. Since no bonds are broken while performing such a move, the sequence of beads in the chain and its length are preserved.

Complementary to ref 26, in the present paper, the length of the matrix elements is gradually varied from $N = 1$ (solvent molecules) to $N = N_g$ (polymers identical to the grafted ones). In the studies we concentrate on systems containing chains end-grafted onto the outer surface of a sphere as well as on a hard wall. The latter is represented by a two-dimensional set of lattice sites resulting from breaking the periodic boundary conditions in one direction.

The simulation parameters include the surface coverage σ, sphere radius R, and the lengths N_g and N of the end-grafted and matrix chains, respectively. The coverage σ is defined as

$$\sigma = n_g/n_s \tag{1}$$

where n_g is the number of the end-grafted chains and n_s stands for the total number of lattice sites representing the spherical surface. A lattice site belongs to the spherical surface if it does not belong to the sphere but at least one of its 12 neighbors does.

The simulated systems are characterized by means of the monomer concentration profile of the end-grafted polymers as a function of the distance from the surface, $\rho_m(z)$, defined as

$$\rho_m(z) = \langle n_m \rangle(z)/n_{latt}(z) \tag{2}$$

where $\langle n_m \rangle(z)$ denotes the average number of the end-grafted polymer beads with distance to the interface between z and $z + \Delta z$, and $n_{latt}(z)$ is the total number of the lattice sites in this layer. The concentration profile of the free ends, $\rho_{fe}(z)$, of the grafted chains is defined similarly

$$\rho_{fe}(z) = \langle n_e \rangle(z)/n_{latt}(z) \tag{3}$$

with $\langle n_e \rangle(z)$ standing for their average number. The calculation of concentration profiles is complemented by examining the distribution of polymer centers of mass, $\langle n_{cm} \rangle(z)$, related to the layer volume, $V(z)$

$$\rho_{cm}(z) = \langle n_{cm} \rangle(z)/V(z) \tag{4}$$

The monomer concentrations of grafted and free chains at any z are such that their sum is always one.

Results

In the first part of the presentation of our results, we concentrate on the influence of various σ and R on the properties of the grafted chains in various environments (see Figure 1). The schematic pictures shown refer to the two limiting types of matrices surrounding the hairy sphere: a pure solvent of single beads $N = 1$ and a dense melt of identical polymers $N = N_g$.

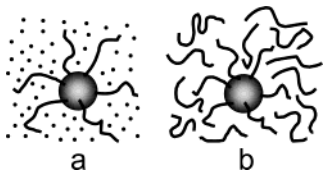

Figure 1. Schematic illustration of the extreme cases of the considered model systems: the hairy sphere in a good low molecular solvent (a) and in a polymer melt (b).

In Figure 2a,b the monomer concentration profiles $\rho_m(z)$ of the grafted chains are plotted vs distance z from the sphere surface for $N_g = 50$, $\sigma = 1$, 0.8, 0.69, 0.5, 0.2, and for two different values of the sphere radius $R = 3$ and 10. Subsequently, in Figure 2c we present $\rho_m(z)$ determined in the limiting case of a flat wall ($R \to \infty$). In agreement with the earlier molecular dynamics simulations of linear chains attached to a flat surface,[31] the figures well indicate that $\rho_m(z)$ monotonically increases with increasing σ and decreases with z for fixed values of the other parameters. It is true for both the simple solvent and a highly concentrated melt. Figure 2b,c also indicates that in the case of the melt and for sufficiently high σ there is a finite layer where the monomer concentration of the anchored chains is both large and almost constant. This means that under such conditions the free polymers are practically prevented from exploring the neighborhood of the surface. Moreover, the profiles change from concave to convex as the curvature of the sphere decreases. It is also worth noticing that for the chains grafted to the surfaces with $R = 10$ and ∞ and immersed in the good solvent ($N = 1$) there exists a depletion of ρ_m near the surface that is better pronounced for smaller σ (e.g., $\sigma = 0.2$). Such a transition to a parabolic-type profile accompanied by a decrease in the monomer concentration near the surface has already been reported in the papers concerned with off-lattice Monte Carlo simulations.[36,37] The effect equivalent to the saturation of density near the grafting surface has also been observed in simulated melts of multiarm stars,[38] which one can consider as hairy spheres with extremely small core. For the stars with number of arms exceeding nearly 25 an intramolecular density reaching density of a bulk system has been observed.

In Figure 3 we have compared the simulation results obtained for the smaller hairy sphere $R = 3$ immersed in various melts (various N) with the scaling predictions proposed for star polymers in high molecular weight solvents.[28] The theory argues that close to the star center

$$\rho_m(r) \approx 1 \tag{5a}$$

whereas at larger distances r from it

$$\rho_m(r) \sim r^{-4/3} n_g^{2/3} N^{1/3} \tag{5b}$$

As indicated by the figure, we do not find a satisfactory agreement with the theoretical formulas. Actually, even in the linear scale, there are no clear intervals of $(r/N_g)^{-4/3}$ within the layers, where the curves could be

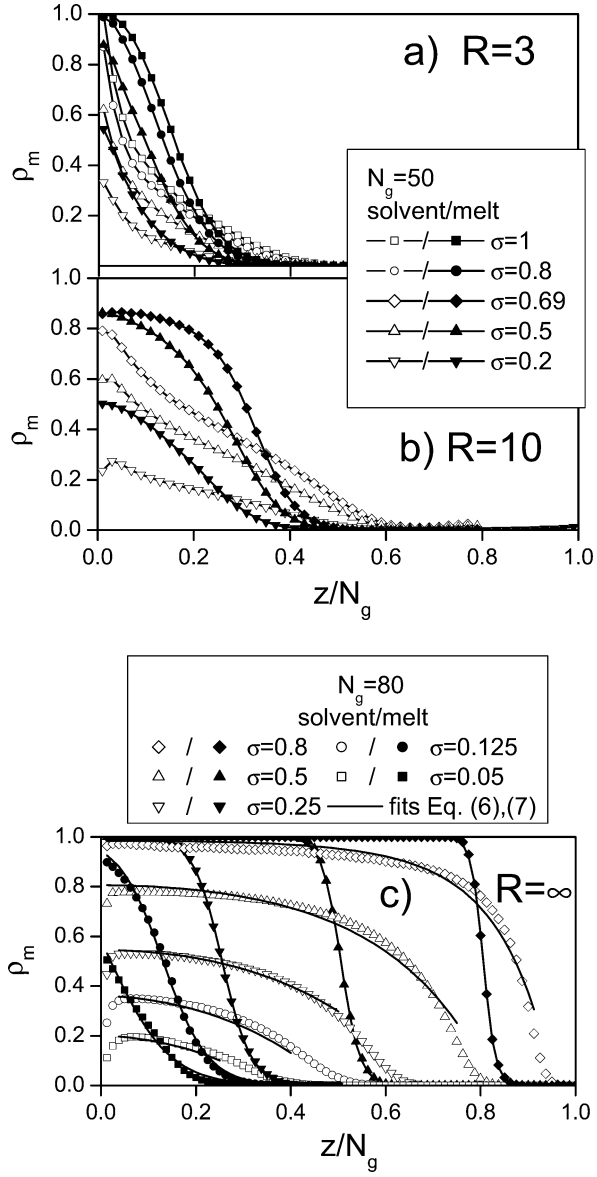

Figure 2. (a) Monomer concentration profiles $\rho_m(z)$ as a function of the distance z from the sphere surface in a pure solvent ($N = 1$) and dense melt ($N = N_g$) for chains with $N_g = 50$ grafted to the sphere with the radius $R = 3$ and for various σ. (b) Same as in (a) except $R = 10$. (c) Same as in (a) except $N_g = 80$, $R \rightarrow \infty$; continuous lines are fits defined by eqs 6 and 7.

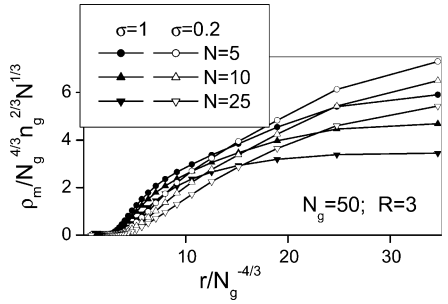

Figure 3. Test of the scaling relation for the "hairy sphere" of radius $R = 3$ in the melts of chains with various N.

considered straight lines. We can only argue that the scaling relations are better approached for smaller values of N.

In the hard wall case, in turn, the hyperbolic tangent form

$$\rho_m(z) = \{1 - \tanh[(z - h)/q]\}/2 \tag{6}$$

(with h and q as the parameters) provides almost a perfect fit to the data for the grafted chains in a melt of long free chains ($N = N_g$) and a wide range of higher σ ($\sigma \geq N_g^{-1/2}$),[18,29,30] as shown in Figure 2c. In the other extreme of a simple neutral solvent ($N = 1$) the SCF exponential function[12−14]

$$\rho_m(z) = 1 - \exp[-k^2(h^2 - z^2)] \tag{7}$$

(with h and k as the parameters) provides a reasonable fit to the concentration profile in the "scaling regime" for almost all σ as well. However, unlike the theoretical prediction concerning k, we find that this parameter does reveal some dependence on σ. A number of examples of the fitting curves are shown in Figure 2c by continuous lines.

Next, we turn to test the scaling relations for the brush width and penetration length of the melt into the flat brush. This has been done in two ways: by using the fitting formulas (6) and (7) (a) and by direct graphical differentiation and integration of the simulated concentration distributions (b). Actually, h in (6) and (7) and $2q$ in (6) are interpreted as the brush height and penetration length, respectively, and as such can be directly read out from the fits.[12−14,18] The penetration length of the simple solvent into the grafting layer can, in turn, be determined from the definition[18]

$$\lambda = -\{\partial\rho_{\text{fit}}/\partial z\}^{-1}_{\rho=0.5} \tag{8}$$

On the other hand, less formally, h can also be determined by graphical integration

$$h = 2\frac{\int_0^\infty \rho_m z \, dz}{\int_0^\infty \rho_m \, dz} \tag{9}$$

whereas λ by graphical differentiation of the simulated concentration profiles using (8).

The results obtained in such ways for fixed N_g are presented in Figure 4. The scaling relations predicted for h and λ read

$$h \sim \sigma^{\alpha} \tag{10a}$$

$$\lambda \sim \sigma^{\beta} \tag{10b}$$

with $\alpha = 1$, $\beta = -1/3$ in the dry brush and long chain solvent regime, and $\alpha = 1/3$, $\beta = -1$ in the wet stretched brush regime.[9,30,31] As indicated in Figure 4a, the relation (10a) is well-fulfilled for both regimes. Only for the smallest σ some discrepancy from linearity is present for the dry brush and long chain solvent case using eq 9. With respect to λ (Figure 4b), the obtained results might be considered linear in the logarithmic scale only for the dry brush regime, though the exponents are different from the theoretical values. Actually, a linear fit to the points obtained with (8) leads to $\beta \approx -0.65$, whereas to the ones found with (6) $\beta \approx -0.55$. In the other case, with the use of (8) and the differential function of (7), the obtained scaling behavior of λ is entirely different from that predicted theoretically. Actually, clear discrepancies from linearity are well seen, and we find that in the limit of very dense grafting the penetration length of the solvent into the layer is

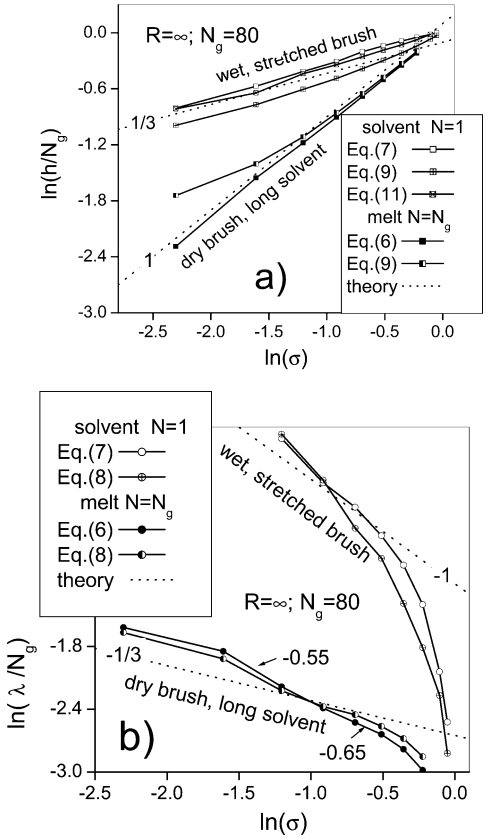

Figure 4. Tests of the various scaling predictions concerning (a) the width of the flat grafted layer, h, and (b) the penetration length of the mobile molecules into the brush, λ.

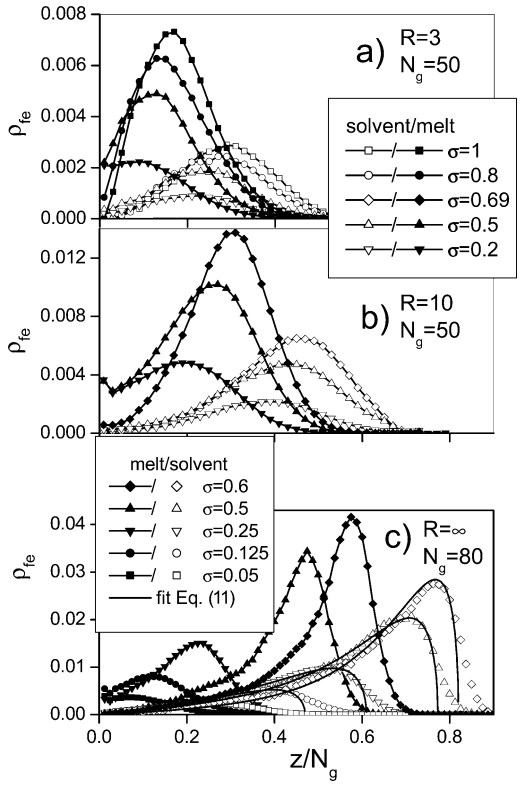

Figure 5. (a) Concentration of the free ends $\rho_{fe}(z)$ as a function of the distance z from the sphere surface in a pure solvent ($N = 1$) and dense melt ($N = N_g$) for chains with $N_g = 50$ grafted to the sphere with the radius $R = 3$ and for various coverage σ. (b) Same as in (a) except $R = 10$. (c) Same as in (a) except $N_g = 80$, $R \to \infty$; continuous lines are fits defined by eq 11.

smaller than foreseen by the scaling formula. Thus, we do not find a satisfactory, quantitative confirmation of the scaling relations describing the penetration length. In the dry brush and long solvent regime the agreement might only be seen as qualitative. The discrepancy results primarily from the incorrect limits which the scaling relations predict for the range of σ approaching 1. The penetration length should in this range become 0. Simulation results show clearly this tendency, but according to the scaling laws nonzero values are expected. Increasing chain length in the simulated systems can probably improve the agreement with the scaling prediction in the range of small σ but cannot remove the discrepancy completely.

Next, we describe the free chain-ends concentrations $\rho_{fe}(z)$ that are shown in Figure 5a−c for various R and σ. In accordance with the earlier observations,[36,37] their shape is such that they are no longer monotonic functions of z but grow from low values near the grafting surface up to a clear maximum at some z and subsequently drop to zero. Both for the good solvent and for the melt, the larger σ the higher maximum located further away from the surface. Furthermore, in some cases of the melt matrix and lower surface coverage, the concentration of the free ends is finite at the surface.

For the flat layer in the pure solvent we have fitted ρ_{fe} with the SCF function of the form

$$f(z) = gz \exp[-k^2(h^2 - z^2)](h^2 - z^2)^{1/2}\Theta(z - h) \quad (11)$$

(g, k, h = the fitting parameters) which comes from the approximation of the Dawson integral $D(t)$[12]

$$D(t) \approx \exp(-t^2)t \quad (12)$$

Equation 11 provides a very good fit to the computed distributions of grafted chain ends for a wide range of σ indeed. Some examples of the curves obtained in such a way are shown in Figure 5c, whereas $\ln(h/N_g)$, interpreted as the brush width, vs $\ln(\sigma)$ is also included in Figure 4a. One can see again that (11), (7), and (9) bring about very similar scaling behavior of the brush width. However, unlike the theoretical result, we find again that the parameter k reveals some dependence on σ.

In Figure 6a,b we show the distributions of the grafted−-polymer centers of mass $\rho_{cm}(z)$ (CM profiles) for $R = 3$, 10 and for various σ. Similarly to the concentration of the free ends, ρ_{cm} raise from nearly zero at the particle surface up to a clear maximum and then go down to zero again with increasing z for the given R, N_g, N, and σ. The figures also present that the CM profiles reveal a strong monotonic dependence on σ for larger values of which are sharper with higher maximum. Furthermore, as for ρ_{fe}, the resulting distributions possess higher maxima with positions shifted toward the particle surface for the melt matrix. All of these observations correspond with the results obtained for the hard wall system shown in Figure 6c.

In the rest of the paper, the effect of varying chain length N of the matrix on the anchored polymers is presented in a bit more detail. In Figure 7a,b the concentration profiles $\rho_m(z)$ of the grafted chains are plotted vs distance z from the sphere surface for $N_g = 50$, $\sigma = 1$, 0.69, 0.2, $N = 1$, 5, 10, 25, 50, and for two different values of the sphere radius R. The effect of varying the solvent chain length N on $\rho_m(z)$ is such that, for higher surface coverage $\sigma = 1$ and 0.69, the profiles

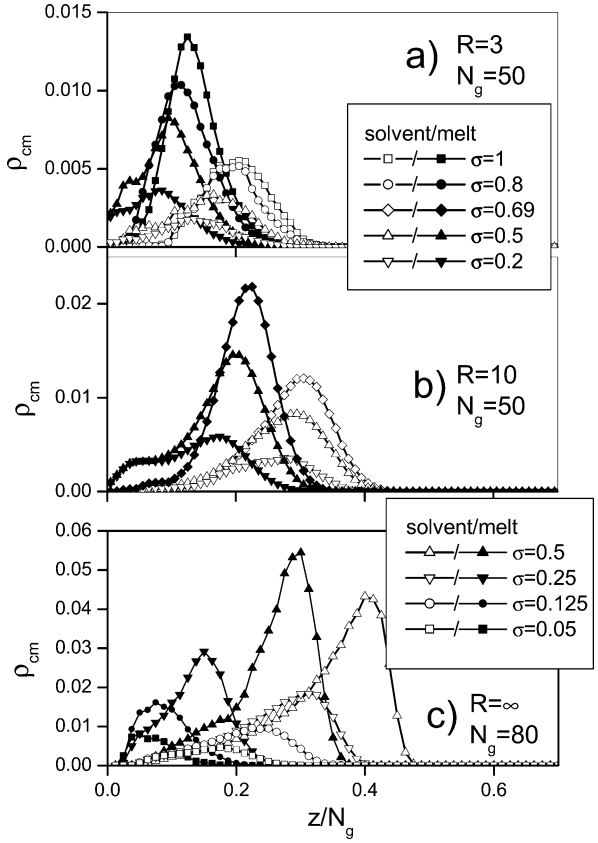

Figure 6. (a) CM concentration $\rho_{cm}(z)$ as a function of the distance z from the sphere surface in a good solvent ($N = 1$) and dense melt ($N = N_g$) for chains with $N_g = 50$ grafted to the sphere with the radius $R = 3$ and for various coverage σ. (b) Same as in (a) except $R = 10$. (c) Same as in (a) except $N_g = 80$, $R \rightarrow \infty$.

change from concave in the case of $N = 1$ to convex for the melt matrix with $N = N_g$. They do not change their shape so dramatically for smaller $\sigma = 0.2$, though some effect of N is also present. Actually, it is worth noticing that, for the chains grafted to the larger sphere and immersed in the good solvent ($N = 1$), there exists a depletion of the monomer concentration near the particle surface (e.g., $\sigma = 0.2$) which disappears with increasing N. Subsequently, the consideration of the monomer concentration profiles is complemented with Figure 7c, where ρ_m for $N_g = 80$, $\sigma = 0.25$ and for various lengths of matrix chains, N, are shown in the limiting case of a flat wall ($R \rightarrow \infty$). The observed influence of N on the brush density profiles is similar to what is found for the interface with the finite radius $R = 10$ and $\sigma = 0.2$. In particular, a depletion of the monomer concentration is seen only for the simple solvent conditions.

Next, we analyze the free chain-ends concentrations, $\rho_{fe}(z)$, which are shown in Figure 8a,b for $R = 3$, 10 and for $\sigma = 1$, 0.2. The pictures indicate how the medium in which the hairy sphere is immersed influences the profiles of free ends of the grafted chains. Actually, for both the larger and smaller sphere, the observed tendency is such that the larger N the higher maximum that is located closer the sphere surface. In particular, this is also the case for chains grafted to a flat surface, which is presented in Figure 8 c. Furthermore, for $N = N_g$, $R = 10$, and $R \rightarrow \infty$, the concentration of the free ends is finite even at the surface, which means that a small fraction of the ends concentrate in that region. This crates grafted chain loops. The observations made

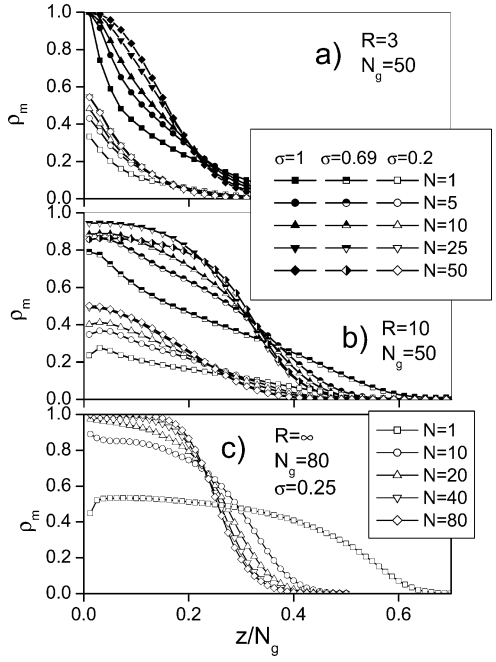

Figure 7. (a) Monomer concentration profiles $\rho_m(z)$ as a function of the distance z from the sphere surface for chains with $N_g = 50$ grafted to the sphere with the radius $R = 3$ for various N and σ. (b) Same as in (a) except $R = 10$. (c) Same as in (a) except $N_g = 80$, $R \rightarrow \infty$.

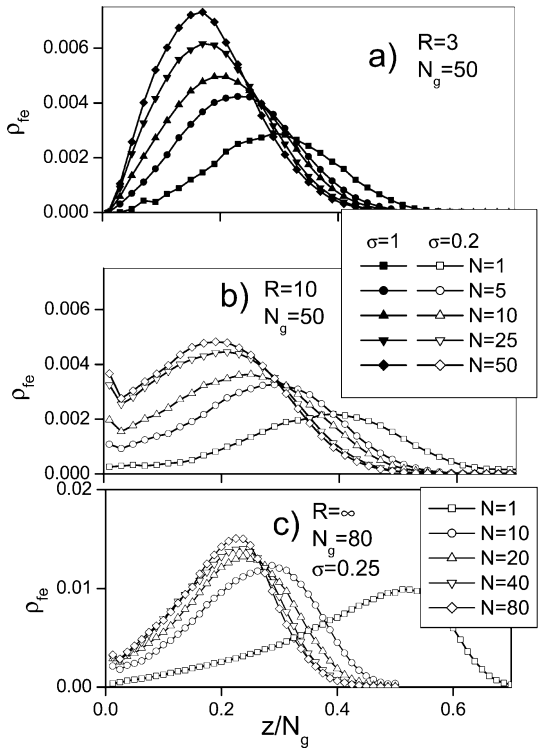

Figure 8. (a) Concentration of the free ends $\rho_{fe}(z)$ as a function of the distance z from the sphere surface for chains with $N_g = 50$ grafted to the sphere with the radius $R = 3$ for various N and σ. (b) Same as in (a) except $R = 10$. (c) Same as in (a) except $N_g = 80$, $R \rightarrow \infty$.

for ρ_{fe} and ρ_m are again in qualitative agreement with the findings of ref 31, though we do not see oscillations of ρ_m in the vicinity of the surface (due to the fact that our simulations are performed on the lattice).

In Figure 9a,b we show the CM distributions for the grafted-polymers for $R = 3$, 10 and for $\sigma = 1$, 0.69, 0.2. The observed effect of various N on the distributions of

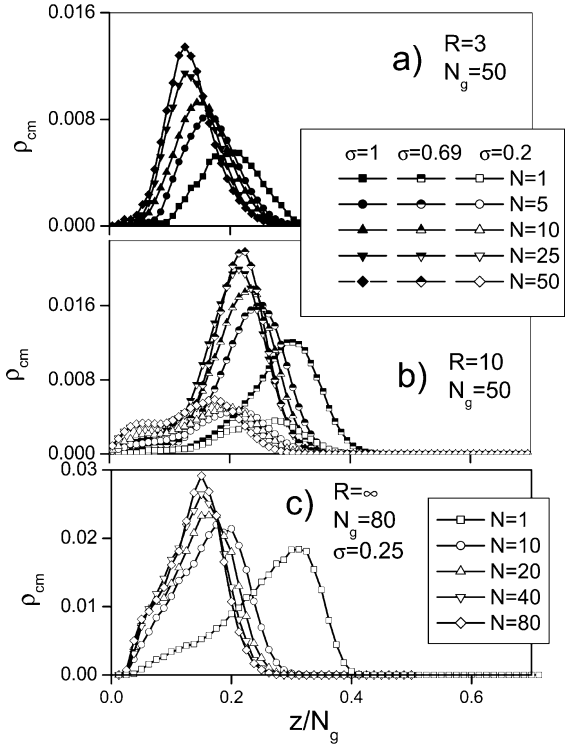

Figure 9. (a) CM concentration $\rho_{cm}(z)$ as a function of the distance z from the sphere surface for chains with $N_g = 50$ grafted to the sphere with the radius $R = 3$ for various N and σ. (b) Same as in (a) except $R = 10$. (c) Same as in (a) except $N_g = 80$, $R \to \infty$.

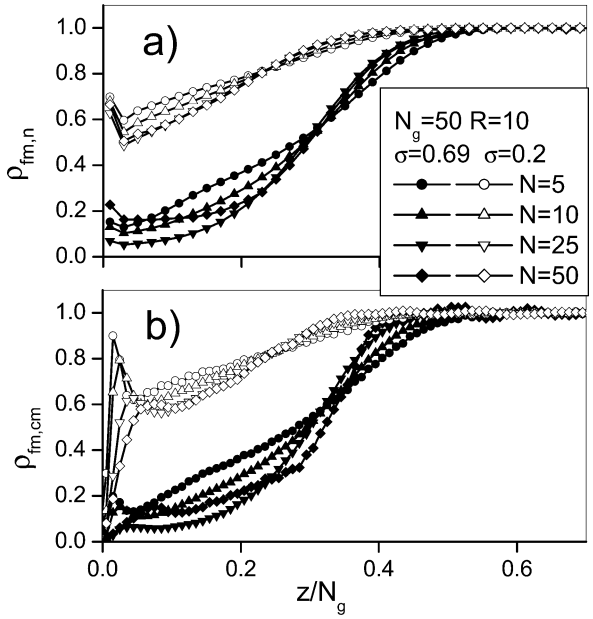

Figure 10. (a) Normalized concentration of the chain ends $\rho_{fm,n}(z)$ of the matrix chains as a function of the distance z from the surface of the grafting sphere with $R = 10$ for various σ and N. (b) Center-of-mass profile $\rho_{fm,cm}(z)$ of the matrix chains as a function of the distance z from the surface of the same sphere as in (a) for various σ and N.

the chain centers of mass is again similar to that for the free ends. Actually, the anchored polymers immersed in the dense melt are more compressed, and as a result, most of their CM points concentrate closer to the interface. This is also the case for the flat grafted layer shown in Figure 9c.

Next, in Figure 10a,b, we present some properties of the chains that constitute the "medium" surrounding the hairy sphere. In particular, we concentrate on the normalized distributions of their ends $\rho_{fm,n}(z)$ and centers of mass $\rho_{fm,cm}(z)$. Briefly speaking, Figure 10a indicates that $\rho_{fm,n}$ decreases its value as z approaches the particle surface; i.e., to some extent the chains constituting the matrix are prevented from exploring the neighborhood of the sphere by the grafted ones. This kind of effect is more pronounced for higher values of σ. Moreover, in the extreme of small surface coverage, $\rho_{fm,n}$ does not drop monotonically but reveals an increase for z close to 0. The effect of N on the profiles is such that very near the sphere the longer the matrix chains the lower the concentration of their ends, though there is an exception to that rule for $\sigma = 0.69$, $N = 25$, 50. Qualitatively, the behavior of the CM profiles $\rho_{fm,cm}$ shown in Figure 10b resembles that of $\rho_{fm,n}$ with the difference that they fall down to zero from a local maximum in the vicinity of the interface. The effect of maxima in the CM profiles for the matrix chains in the range of low z indicates a kind of trapping of these chains near the particle surface.

Summary

Using the cooperative motion algorithm, we have performed simulations of linear polymers end-grafted to a spherical surface as well as to a flat wall considered as a limiting case ($R = \infty$). For various values of the radius of the grafting sphere, surface coverage, and chain lengths, we have examined concentration profiles of chain monomers, free chain ends, and chain centers of mass. In agreement with the other simulation studies, we have found that these quantities are sensitive to changes of the interface radius, the surface coverage, and the surrounding matrix. For instance, as the curvature of the interface decreases, the monomer concentration profiles approach the case of a flat grafting plate. Furthermore, there is a depletion of this quantity near the surface for the matrix of single beads and for low surface coverage. Subsequently, with respect to the concentrations of the free chain ends and centers of mass, we have found that they reveal clear maxima at some distance from the particle surface. The shape and height of the latter, for the fixed chain length, are determined by the surface coverage, too.

We have also fitted the data with various theoretical formulas describing the monomer concentration profiles and concentration of the free chain ends for the dry brush long solvent regime and stretched wet brush regime for the impenetrable grafting plane. The fitting parameters along with the data itself were than used to checked out the scaling relations with respect to the layer width and the penetration length of the melt into the layer. Whereas, the former corresponds very well with the theory quantitatively, the latter does not, and the correspondence might be seen as only qualitative.

Special attention has been paid to inspecting the effect of changing matrix parameters. The length of the polymers constituting the media has also been considered as a variable with the limits $N = 1$ and $N = N_g$ referring to the two extremes of a good simple solvent and a polymer melt, respectively. Among others, our simulations have well shown that for longer matrix chains the anchored ones reveal a tendency to take more shrunken forms, i.e., to concentrate in the vicinity of the interface. This kind of conclusion is supported by the observation that the maximal values of the free ends

and CM profiles undergo a shift toward the surface as N increases.

Finally, with the respect to various N and σ, we have examined the properties of the free chains constituting the surrounding media. Especially for high surface coverage, these chains are prevented from exploring the neighborhood of the surface. As a result, a reduction in the number of chain ends and the centers of mass has been found. Moreover, some influence of changing N is also present.

Acknowledgment. This work was supported by the European Community Research Training Network HUSC (From Hard to Ultrasoft Colloids) under Contract HPRN-CT-2000-00017.

References and Notes

(1) Jones, R. A. L.; Norton, L. J.; Shull, K. R.; Kramer, E. J.; Felcher, G. P.; Karim, A.; Fetters, L. J. *Macromolecules* **1992**, *25*, 2359.
(2) Clarke, C. J.; Jones, R. A. L.; Edwards, J. L.; Shull, K. R.; Penfold, J. *Macromolecules* **1995**, *28*, 2042.
(3) Hasegawa, R.; Aoki, Y.; Doi, M. *Macromolecules* **1996**, *29*, 6656.
(4) Henn, G.; Bucknall, D. G.; Stamm, M.; Vanhoorne, P.; Jérôme, R. *Macromolecules* **1996**, *29*, 4305.
(5) Reiter, G.; Schultz, J.; Auroy, P.; Auvray, L. *Europhys. Lett.* **1996**, *33*, 29.
(6) Kerle, T.; Yerushalmi-Rozen, R.; Klein, J. *Europhys. Lett.* **1997**, *38*, 207.
(7) Alexander, S. *J. Phys. (Paris)* **1977**, *38*, 977.
(8) de Gennes, P. G. *Macromolecules* **1980**, *13*, 1069.
(9) Gay, C. *Macromolecules* **1997**, *30*, 5939.
(10) Auboy, M.; Raphaël, E. *Macromolecules* **1994**, *27*, 5182.
(11) Auboy, M.; Fredrickson, G. H.; Pincus, P.; Raphaël, E. *Macromolecules* **1995**, *28*, 2979.
(12) Zhulina, E. B.; Borisov, O. V.; Brombacher, L. *Macromolecules* **1991**, *24*, 4679.
(13) Wijmans, C. M.; Scheutjens, J. H. M.; Zhulina, E. B. *Macromolecules* **1992**, *25*, 2657.
(14) Wijmans, C. M.; Zhulina, E. B.; Fleer, G. J. *Macromolecules* **1994**, *27*, 3238.
(15) Witten, T. A.; Leibler, L.; Pincus, P. A. *Macromolecules* **1990**, *23*, 824.
(16) Ferreira, P. G.; Leibler, L. *J. Chem. Phys.* **1996**, *105*, 9362.
(17) Ferreira, P. G.; Ajdari, A.; Leibler, L. *Macromolecules* **1998**, *31*, 3994.
(18) Shull, K. R. *J. Chem. Phys.* **1991**, *94*, 5723.
(19) Shull, K. R.; Kramer, E. *Macromolecules* **1990**, *23*, 4769.
(20) Shull, K. R. *Macromolecules* **1996**, *29*, 2659.
(21) Cosgrove, T.; Heath, T.; van Lent, B.; Leermakers, F.; Scheutjens, J. *Macromolecules* **1987**, *20*, 1692.
(22) Semenov, A. N. *Macromolecules* **1992**, *25*, 4967.
(23) Binder, K.; Lai, P. Y.; Wittmer, J. *Faraday Discuss.* **1994**, *98*, 97.
(24) Zajac, R.; Chakrabarti, A. *Phys. Rev. E* **1994**, *49*, 3069.
(25) Klos, J.; Pakula, T. *J. Chem. Phys.* **2003**, *118*, 1507.
(26) Klos, J.; Pakula, T. *J. Chem. Phys.* **2003**, *118*, 7682.
(27) Ball, R. C.; Marko, J. F.; Milner, S. T.; Witten, T. A. *Macromolecules* **1991**, *24*, 693.
(28) Raphaël, E.; Pincus, P.; Fredrickson, G. H. *Macromolecules* **1993**, *26*, 1996.
(29) Borukhov, I.; Leibler, L. *Phys. Rev. E* **2000**, *62*, R41.
(30) Borukhov, I.; Leibler, L. *Macromolecules* **2002**, *35*, 5171.
(31) Grest, G. S. *J. Chem. Phys.* **1996**, *105*, 5532.
(32) Pakula, T. Simulations on the Completely Occupied Lattice. In *Simulation Methods for Polymers*; Kotelyanskii, M. J., Theodorou, D. N., Eds.; Marcel-Dekker: New York, 2004; Chapter 5.
(33) Pakula, T. *J. Chem. Phys.* **1991**, *95*, 4685.
(34) Pakula, T.; Zhulina, E. B. *J. Chem. Phys.* **1991**, *95*, 4691.
(35) Pakula, T.; Zhulina, E. B. *Macromolecules* **1992**, *25*, 754.
(36) Toral, R.; Chakrabarti, A. *Phys. Rev. E* **1993**, *47*, 4240.
(37) Lindberg, E.; Elvingson, C. *J. Chem. Phys.* **2001**, *114*, 6343.
(38) Pakula, T. *Comput. Theor. Polym. Sci.* **1998**, *8*, 21. Pakula, T.; Vlassopoulos, D.; Fytas, G.; Roovers, J. *Macromolecules* **1998**, *31*, 8931.

MA049818L